Electronic communication between two [10]cycloparaphenylenes and bisazafullerene $(C_{59}N)_2$ induced by cooperative complexation

Jérémy Rio,[b]§ Sebastian Beeck,[a]§ Georgios Rotas,[c]§ Sebastian Ahles,[a]§ Denis Jacquemin,[d] Nikos Tagmatarchis,*[c] Chris Ewels*[b] and Hermann A. Wegner*[a]

Abstract: The complex of [10]cycloparaphenylene ([10]CPP) with bisazafullerene $(C_{59}N)_2$ is investigated experimentally and computationally. Two [10]CPP rings are bound to the dimeric azafullerene giving [10]CPP⊃$(C_{59}N)_2$⊂[10]CPP. Photophysical and redox properties support an electronic interaction between the components especially with the second [10]CPP bound. Unlike [10]CPP⊃C_{60}, where there is negligible electronic communication between the two species, upon photoexcitation a partial charge transfer phenomenon is revealed between [10]CPP and $(C_{59}N)_2$ reminiscent of CPP encapsulated metallofullerenes. Such an alternative electron-rich fullerene species demonstrates C_{60}-like ground-state properties and metallofullerene-like excited-state properties opening new avenues for construction of functional supramolecular architectures with organic materials.

Supramolecular chemistry can arguably be regarded as the most essential mechanism of life.[1] While Nature brilliantly employs the various concepts in supramolecular chemistry to achieve function, the creation of artificial systems is still hampered by a lack of knowledge to control molecular assemblies.[2] Although tremendous progress has been achieved in recent years,[3] e.g. in the preparation of rotaxanes,[4] knots,[5,6] switches[7] or machines,[8] there are still many unexplored ways to tie and let interact two or more individual molecules together. Besides hydrogen bonding, ion pairing or metal complexes, π-π interactions have recently gained much attention due to the potential in building molecular architectures for electronic applications.[9] Notably, cyclic π-conjugated species composed of multiple aromatic rings, cycloparaphenylenes (CPPs),[10-12] with diameter in the nm range have emerged as model systems to study such π-π-interactions under defined conditions. CPPs represent the smallest armchair carbon nanotube (CNT) segment,[13] hence, offering unique opportunity to gain fundamental insights for the design and preparation of devices with controlled structure, chirality and electronic properties.

[a] Sebastian Beeck, Sebastian Ahles, Prof. Dr. Hermann A. Wegner
Justus Liebig University, Institute of Organic Chemistry
Heinrich-Buff-Ring 17, D-35392 Giessen, Germany
E-mail: Hermann.a.wegner@org.chemie.uni-giessen.de
[b] Jérémy Rio, Dr. Chris Ewels
Institut Des Matériaux Jean Rouxel (IMN) - UMR6502
2 Rue de la Houssinière, BP32229, 44322 Nantes, France
[c] Dr. Georgios Rotas, Dr. Nikos Tagmatarchis
Theoretical and Physical Chemistry Institute
National Hellenic Research Foundation
48 Vassileos Constantinou Avenue, 11635 Athens, Greece
[d] Prof. Denis Jacquemin
Laboratoire CEISAM - UMR CNRS 6230, Université de Nantes
2 Rue de la Houssinière, BP 92208, 44322 Nantes Cedex 3, France,
and Institut Universitaire de France
103 Blvd. Saint-Michel, F-75005 Paris Cedex 05, France
§ These authors contributed equally.

Supporting information for details on spectroscopic studies and calculations for this article is given via a link at the end of the document.

Regarding the supramolecular chemistry of CPPs, only the preparation of a few 1:1 complexes of CPPs with fullerenes has been accomplished. Remarkably, in those complexes, high size-specificity of the CPP, based on the number of conjugated aromatic rings, is identified directly related with the size of the carbon cage.[14-19] For example, in [10]CPP⊃C_{60}, the best fit of [10]CPP, with 1.4 nm diameter, was for C_{60}[14,15] as well as Li@C_{60}[16] and [11]CPP, with 1.5 nm diameter, for C_{70}[17] as well as La@C_{82},[18,19] respectively. Although the association of the CPP species and empty fullerenes is mainly developed via multiple van der Waals forces, in the case of endohedral fullerenes Li@C_{60} and La@C_{82} charge-transfer interactions are also prevalent. Beyond CPPs, the tubular macrocycle [4]cyclo-2,8-chrysenylene was employed to complex with C_{60}[20,21] as well as to form a supramolecular host-guest system with the dumbbell-shaped dimer $(C_{60})_2$ in 2:1 ratio.[22] In the latter supramolecular system, solely consisting of hydrogen and carbon atoms, the high-reliability for the two receptors self-sorted around the dimeric fullerene cages is facilitated by van der Waals interactions.

Motivated by the aforementioned points, the objective of the current work is two-fold, namely to explore different binding modes for CPPs owed to non-covalent aromatic interactions, and to manage charge-transfer processes within the self-assembled architecture (Figure 1). Herein, we expand the scope of encapsulating fullerene cages by CPPs by introducing the dumbbell-shaped bisazafullerene $(C_{59}N)_2$ species as an *N*-doped fullerene analogue of C_{60}, where a carbon atom is replaced by nitrogen.[23]

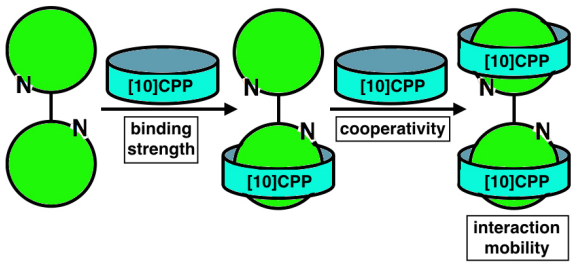

Figure 1. The [10]CPP⊃$(C_{59}N)_2$⊂[10]CPP complex, addressing fundamental questions in supramolecular chemistry of carbon materials.

The formation of the [10]CPP⊃$(C_{59}N)_2$⊂[10]CPP complex was realized by mixing [10]CPP and $(C_{59}N)_2$ in toluene as well as in 1,2-dichlorobenzene (*o*-DCB). Job plot analysis, by plotting spectral changes at the absorption band of [10]CPP centered at 340 nm (Supporting Information, Figure S1), revealed a maximum at a mole fraction of 0.33, hence confirming the stoichiometry for [10]CPP:$(C_{59}N)_2$ as 2:1. Binding constants for the [10]CPP units were calculated and found to be K_1 = 8.4 x 10^6 M^{-1} for the first CPP and K_2 = 3.0 x 10^6 M^{-1} for the second (Supporting Information, Figure S2). The overall binding strength is slightly higher than that of [10]CPP with C_{60},

indicating stable complex formation.[15,16] Markedly, the cooperativity factor α shows a value greater than one (α = 1.45), supporting attractive interactions between the two [10]CPP macrocycles (for calculation see SI).

Additional assays employing variable temperature ^{1}H-NMR-measurements with different ratios of [10]CPP and $(C_{59}N)_2$ were performed to complement the UV-Vis study. Despite the low solubility of $(C_{59}N)_2$, CD_2Cl_2 was the only suitable solvent, which allowed analysis as well as cooling to –40 ºC. At 30 ºC, dynamic behaviour is observed, evidenced by a broad band in the range 7.70-7.45 ppm (Figure 2). Cooling from rt to –20 ºC resulted in distinct, while still broadened, signals. The two larger ones can be assigned to the 1:1 complex [10]CPP⊃$(C_{59}N)_2$. These signals are assigned to the protons pointing to the inside and outside of the fullerene dimer, respectively. Further cooling sharpens these peaks, which appear at 7.60 and 7.46 ppm at –40 ºC. Additionally, four peaks can be distinguished, which correspond to the [10]CPP⊃$(C_{59}N)_2$⊂[10]CPP complex. Increasing the amount of [10]CPP only enlarged the signals for the 1:1 complex until the free [10]CPP is observed (see supporting information). This observation can be rationalized by the different (low) solubilities of the species involved (solubility order in CD_2Cl_2: $(C_{59}N)_2$ < [10]CPP⊃$(C_{59}N)_2$⊂[10]CPP < [10]CPP⊃$(C_{59}N)_2$ < [10]CPP). As the 1:1 complex shows the higher solubility compared to the 2:1 complex it is observed as the major species. Nevertheless, the maximum concentration of the 2:1 complex is already reached with a ratio of [10]CPP:$(C_{59}N)_2$ of 0.5:1 supporting that the 2:1 complex is the most favored one.

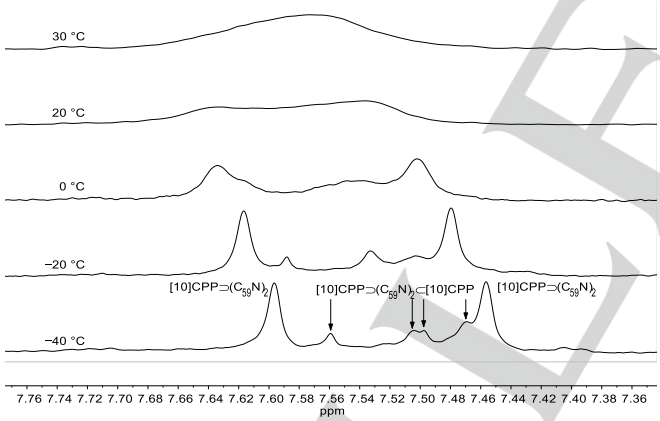

Figure 2. Temperature dependent ^{1}H-NMR assays for the complexation of [10]CPP with $(C_{59}N)_2$ (in CD_2Cl_2).

Local spin density (LDA) density functional (DFT) calculations have been conducted on [10]CPP⊃$(C_{59}N)_2$ revealing an increased binding of 1.89 eV (Figure 3a) compared to [10]CPP⊃C_{60}, consistent with our experimental binding constants, and a net 0.15e charge transfer from [10]CPP to $(C_{59}N)_2$. The calculated migration barrier to exchange between the fullerene cages is rather small (0.2 eV) suggesting the [10]CPP will be mobile between the two fullerenes at rt. The [10]CPP sits on one of the fullerene cages at a 64° angle to the dimer axis. Addition of a second [10]CPP also occurs without a barrier (Figure 3d). While a metastable structure exists with each CPP encapsulating its own fullerene (Figure 3b) there is a strong (1.70 eV) driving force for the CPPs to approach one another (Figure 3c). This asymmetric configuration, with the CPPs at a tilt of 62° and 68° to the fullerene axis, can be rationalized by a subtle interplay of π-π interactions between the phenyl groups and the fullerene cage, C–H-π interactions[24] of the CPP with the other $C_{59}N$-unit as well as maximizing London dispersion interactions between the H-atoms (see supporting information).[25] This is reflected in the calculated charge transfer: while the symmetric structure has a charge transfer of only 0.144 eV per CPP to the dimer, the tilted asymmetric ground state shows a transfer of 0.188 and 0.228 eV for the lower and upper CPP respectively, significantly higher than for the single CPP. With a calculated binding enthalpy of 2.47 eV/CPP, this structure represents the system ground state for [10]CPP⊃$(C_{59}N)_2$⊂[10]CPP.

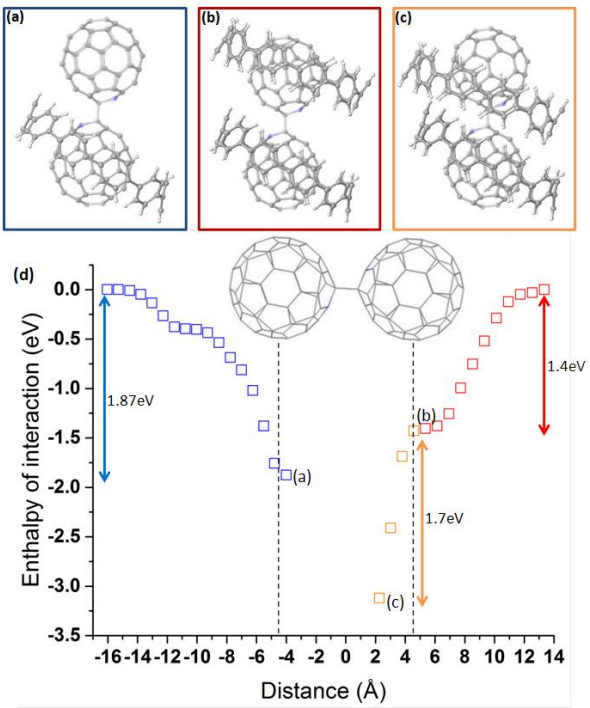

Figure 3. (a) [10]CPP⊃$(C_{59}N)_2$ (b) [10]CPP⊃$(C_{59}N)_2$⊂[10]CPP in metastable symmetric configuration (c) [10]CPP⊃$(C_{59}N)_2$⊂[10]CPP in stable asymmetric configuration. (d) Calculated barriers for insertion of $(C_{59}N)_2$ into single (left) and then second (right) [10]CPP, x-axis shows distance between the CPP ring centres and centre of the $(C_{59}N)_2$ dimer, dotted lines indicate centres of the two $C_{59}N$ fullerenes 9.05 Å apart (show in grey), y-axis gives energy difference compared to isolated [10]CPP (eV).

Electrochemical measurements conducted by differential pulsed voltammetry (DPV) were used to establish the redox characteristics of the [10]CPP⊃$(C_{59}N)_2$⊂[10]CPP complex. Initially, DPV of free [10]CPP in *o*-DCB revealed an oxidation peak at 0.88 V (Figure 4). On addition of 0.25 equiv. $(C_{59}N)_2$, a broad oxidation signal appeared, which upon addition of further $(C_{59}N)_2$ resulted in the evolution of two peaks, at 0.68 V and

0.84 V. When excess of $(C_{59}N)_2$ was added, the peak at 0.68 V became stronger than that at 0.88 V. Overall, considering the [10]CPP⊃$(C_{59}N)_2$⊂[10]CPP complex, the [10]CPP oxidation potential was cathodically shifted by ca. 40 mV, corroborating the easier oxidation of [10]CPP when complexed with the azafullerene. This behaviour is in contrast to the [10]CPP⊃C_{60} but compares to 20 mV shift observed for Li@C_{60}[16] confirming the development of charge-transfer phenomena from the CPP to azafullerene seen in the calculations. Interestingly, a second oxidation peak, at even less positive potentials developed corresponding to the oxidation of the second CPP of the [10]CPP⊃$(C_{59}N)_2$⊂[10]CPP complex, which shows increased charge transfer with its fullerene host, in agreement with our calculated charge states of the [10]CPP pair on the dimer.

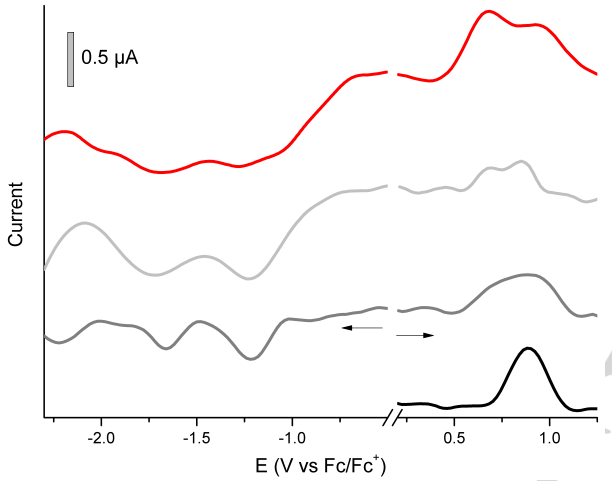

Figure 4. Differential pulse voltammograms of the [10]CPP⊃$(C_{59}N)_2$⊂[10]CPP complex, obtained in *o*-DCB, as formed upon mixing [10]CPP:and $(C_{59}N)_2$ at 1:0 (black), 1:0.25, (dark grey), 1:1 (light grey) and 1:2 (red) equivalents.

This splitting is also reflected in the HOMO and LUMO states (Figure 5). While the HOMO and LUMO of the complex are spatially separated on the CPPs and azafullerene respectively, matching the behaviour for the complex [10]CPP⊃C_{60}, there is an upwards shift compared to the separate component units introducing a splitting of the CPP states. The azafullerene-centred reduction peaks were also identified on the [10]CPP⊃$(C_{59}N)_2$⊂[10]CPP complex, at -1.21, -1.66 and -2.22 V. This anodical shift with respect to those observed for free $(C_{59}N)_2$ shows the more facile reduction processes of azafullerene when complexed with [10]CPP. Notably, the redox potentials for [10]CPP⊃C_{60} remained unaffected for both [10]CPP and C_{60},[16] contrasting the current case, which would be better described as a polarized [10]CPP$^{\delta+}$⊃$(C_{59}N)_2^{\delta-}$⊂[10]CPP complex. At high $(C_{59}N)_2$ concentrations, azafullerene aggregates were formed, thus the reduction waves due to $C_{59}N$ become unresolved (see Figure 4, when [10]CPP:$(C_{59}N)_2$ = 1:2).

Figure 5. Variation in the HOMO (solid) and LUMO (dotted) eigenvalues (eV)

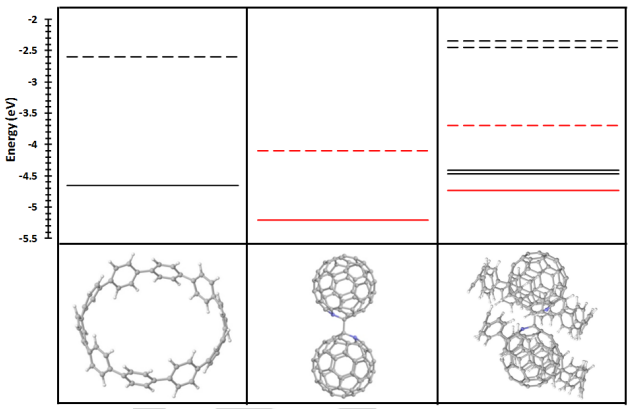

for (a) [10]CPP (black lines), (b) $(C_{59}N)_2$ (red lines) and (c) [10]CPP⊃$(C_{59}N)_2$⊂[10]CPP. Only HOMO-LUMO levels for each subunit are shown, there are additional $(C_{59}N)_2$ states between the LUMOs of $(C_{59}N)_2$ and [10]CPP.

Photoluminescence studies were carried out to investigate the electronic interactions at the excited states within the [10]CPP⊃$(C_{59}N)_2$⊂[10]CPP complex. Photoexcitation at 376 nm, [10]CPP led to a characteristic emission pattern due to different vibrational levels of the ground electronic states (Figure 6). Upon titration of [10]CPP with $(C_{59}N)_2$, the emissive band centred at 472 nm became gradually quenched and blue-shifted by 2, 3 and 7 nm upon additions of 0.5, 1.0 and 2.0 equiv. of $(C_{59}N)_2$, respectively (stronger in toluene in comparison to the more polar *o*-DCB solvent, see supporting information, Figure S3). The latter establishes the effective development of electronic interactions between the two species, within the [10]CPP⊃$(C_{59}N)_2$⊂[10]CPP complex, in the excited state. Notably, the absence of emission in the NIR range, i.e. 800-950 nm, corresponding to the azafullerene emission,[26,27] implies weak, if any, singlet-singlet energy transfer from [10]CPP to $(C_{59}N)_2$. While full TDDFT calculations are not possible on systems of this size, the PL response is consistent with our calculated 4.3 nm blue-shift in HOMO-LUMO gap for the dimer complexed [10]CPP (Figure 5).

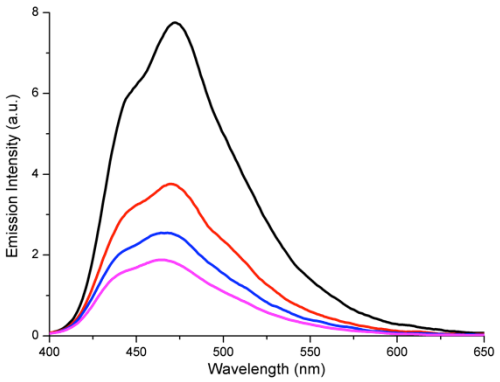

Figure 6. Steady state emission spectra (λ_{ex} = 340 nm) of a 5x10^{-7} M [10]CPP in toluene (black), upon incremental additions of 0.5 (red), 1.0 (blue) and 2.0 (magenta) equivalents of $(C_{59}N)_2$.

Concomitantly, emission decay studies based on the time-correlated single-photon-counting method were performed. The evaluation of the time profile of the photoluminescence decay at 472 nm for the single excited state of ^{1}([10]CPP)* was mono-exponentially fitted with a lifetime of 4.5 ns. However, the decay component in [10]CPP⊃$(C_{59}N)_2$⊂[10]CPP, which corresponds to the quenching of the emission intensity in the steady-state spectrum was not observed. Implicitly, the latter suggests that singlet excited state deactivation of ^{1}([10]CPP)* within the [10]CPP⊃$(C_{59}N)_2$⊂[10]CPP complex is faster than the 50 ps time resolution of our instrumentation.

In conclusion, we show that bisazafullerene $(C_{59}N)_2$ can be complexed by two [10]CPP macrocycles, with the first one stabilizing the binding of the second by maximizing π-π, C–H-π as well as attractive London dispersion interactions, forming [10]CPP⊃$(C_{59}N)_2$⊂[10]CPP. Theoretical simulations reveal an unexpected tilted structure with an asymmetric arrangement of the [10]CPPs on the $(C_{59}N)_2$. Moreover, electrochemical as well as photoluminescence studies deliver meaningful insight for the electronic communication. Redox assays reveal the presence of reduction processes centred at the azafullerene part in [10]CPP⊃$(C_{59}N)_2$⊂[10]CPP and two distinct oxidations due to [10]CPP. The emission of [10]CPP found quenched upon complexation with the azafullerene, confirming the occurrence of charge-transfer phenomena from [10]CPP to $(C_{59}N)_2$ in good agreement with the theoretical modelling. This is the first neutral fullerene-CPP species to demonstrate such strong charge transfer effects. This behaviour is reminiscent of the metallofullerene $Li^+@C_{60}$, with similar positive charge delocalization to the exterior CPPs when encapsulated, however, with much easier accessibility. The efficient fluorescence depression of the emission of [10]CPP in the [10]CPP⊃$(C_{59}N)_2$⊂[10]CPP complex suggests the development of intra-complex electronic interactions in the excited state. In general the unique arrangement in [10]CPP⊃$(C_{59}N)_2$⊂[10]CPP is expected to bring new potential in the area of supramolecular material science of π-systems.

Experimental

Self-assembled [10]CPP ⊃ $(C_{59}N)_2$ ⊂ [10]CPP complex formation monitored by absorption and fluorescence titrations: The [10]CPP[28] (0.74 mg, 0.97 μmol) was dissolved in 100 mL toluene (9.7 μM) and 0.1 mL of this solution (0.097 μmol) was diluted to a final volume of 10 mL (0.97 μM). Also, $(C_{59}N)_2$ (1.47 mg, 1.02 μmol) was dissolved in 100 mL toluene (10.2 μM). Then, 3 mL of the diluted [10]CPP toluene solution was placed into a cuvette and the $(C_{59}N)_2$ toluene solution was added in 15 μL increments. The UV-Vis and fluorescence spectra were measured each time. The formation of [10]CPP⊃$(C_{59}N)_2$⊂[10]CPP, in a [10]CPP to $(C_{59}N)_2$ at a 2:1 stoichiometry, was proved by Job plot analysis following changes in the absorption band of [10]CPP-$(C_{59}N)_2$-mixture centred at 340 nm.

Acknowledgements

This project has received funding from the European Union's Horizon 2020 Research and Innovation Programme under the Marie Sklodowska-Curie grant agreement N° 642742. Calculations were performed at the CCIPL Centre de Calcul Intensif Pays de la Loire. DJ, JR and CE acknowledge Pays de la Loire Paris Scientifiques project "NEWTUBE".

Keywords: cycloparaphenylenes • azafullerene •supramolecular chemistry • photophysics • redox

[1] J.-M. Lehn, *Angew. Chem. Int. Ed.* **2013**, *52*, 2836–2850.
[2] A. Coskun, M. Banaszak, R. D. Astumian, J. F. Stoddart, B. A. Grzybowski, *Chem. Soc. Rev.* **2012**, *41*, 19–30.
[3] F. E. D. E. R. Niess, V. Duplan, J.-P. Sauvage, *Chem. Lett.* **2014**, *43*, 964–974.
[4] W. Yang, Y. Li, H. Liu, L. Chi, Y. Li, *Small* **2012**, *8*, 504–516.
[5] S. F. M. van Dongen, S. Cantekin, J. A. A. W. Elemans, A. E. Rowan, R. J. M. Nolte, *Chem. Soc. Rev.* **2014**, *43*, 99–122.
[6] N. C. H. Lim, S. E. Jackson, *J. Phys.: Condens. Matter* **2015**, 1–35.
[7] Ben L Feringa, W. R. Browne, *Molecular Switches*, John Wiley & Sons, **2011**.
[8] J. M. Abendroth, O. S. Bushuyev, P. S. Weiss, C. J. Barrett, *ACS Nano* **2015**, *9*, 7746–7768.
[9] K.-T. Wong, D. M. Bassani, *NPG Asia Materials* **2014**, *6*, e116.
[10] S. E. Lewis, *Chem. Soc. Rev.* **2015**, *44*, 2221–2304.
[11] A.-F. Tran-Van, H. A. Wegner, *Beilstein J. Nanotechnol.* **2014**, *5*, 1320–1333.
[12] H. Omachi, Y. Segawa, K. Itami, *Acc. Chem. Res.* **2012**, *45*, 1378–1389.
[13] Y. Segawa, A. Yagi, K. Matsui, K. Itami, *Angew. Chem. Int. Ed.* **2016**, *55*, 5136–5158.
[14] T. Iwamoto, Y. Watanabe, T. Sadahiro, T. Haino, S. Yamago, *Angew. Chem. Int. Ed.* **2011**, *50*, 8342–8344.
[15] J. Xia, J.W. Bacon, R. Jasti, *Chem. Sci.* **2012**, *3*, 3018-3021.
[16] H. Ueno, T. Nishihara, Y. Segawa, K. Itami, *Angew. Chem. Int. Ed.* **2015**, *54*, 3707–3711.
[17] T. Iwamoto, Y. Watanabe, H. Takaya, T. Haino, N. Yasuda, S. Yamago, *Chem.-Eur. J.* **2013**, *19*, 14061–14068.
[18] T. Iwamoto, Z. Slanina, N. Mizorogi, J. Guo, T. Akasaka, S. Nagase, H. Takaya, N. Yasuda, T. Kato, S. Yamago, *Chem.-Eur. J.* **2014**, *20*, 14403–14409.
[19] Y. Nakanishi, H. Omachi, S. Matsuura, Y. Miyata, R. Kitaura, Y. Segawa, K. Itami, H. Shinohara, *Angew. Chem. Int. Ed.* **2014**, *53*, 3102–3106.
[20] H. Isobe, S. Hitosugi, T. Yamasaki, R. Iizuka, *Chem. Sci.* **2013**, *4*, 1293–1297.
[21] S. Sato, T. Yamasaki, H. Isobe, *Proc. Natl. Acad. Sci. USA* **2014**, *111*, 8374–8379.
[22] T. Matsuno, S. Sato, A. Yokoyama, S. Kamata, H. Isobe, *Angew. Chem. Int. Ed.* **2016**, *55*, 15339–15343.
[23] J. C. Hummelen, B. Knight, J. Pavlovich, R. Gonzalez, F. Wudl, *Science* **1995**, *269*, 1554–1556.
[24] M. Nishio, Y. Umezawa, M. Hirota, Y. Takeuchi, *Tetrahedron* **1995**, *51*, 8665–8701.
[25] a) J.-V. Climent-Medina, A .-J. Perez-Jimenez, M. Moral, E. San-Fabia, J. -C. Sancho-Garcia, *ChemPhysChem* **2015**, *16*, 1520–1528. b)I. Gonzalez-Veloso, J. Rodriguez-Otero, E. M. Cabaleiro-Lago, *Phys. Chem. Chem. Phys.* **2016**, *18*, 31670–31679.
[26] G. Rotas, N. Tagmatarchis, *Chem. Eur. J.* **2016**, *22*, 1206–1214.
[27] G. Rotas, J. Ranta, A. Efimov, M. Niemi, H. Lemmetyinen, N. Tkachenko, N. Tagmatarchis, *Chem. Phys. Chem.* **2012**, *13*, 1246–1254.
[28] J. Xia, J. W. Bacon, R. Jasti, *Chem. Sci.* **2012**, *3*, 3018–3021.

Entry for the Table of Contents

COMMUNICATION

The complex of two [10]cycloparaphenylenes ([10]CPPs) with bisazafullerene $(C_{59}N)_2$ is investigated experimentally and computationally. Photophysical and redox properties support an electronic interaction between the components. This supramolecular organic fullerene assembly demonstrates C_{60}-like ground-state properties and metallofullerene-like excited-state properties opening new avenues for organic materials.

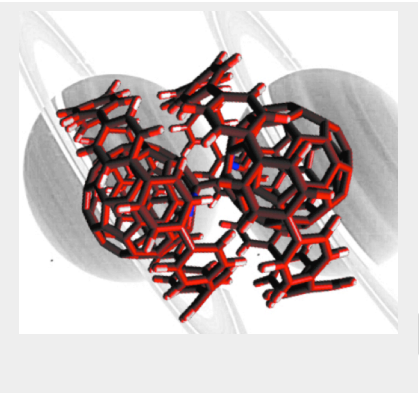

Jeremy Rio, Sebastian Beeck, Georgios Rotas, Sebastian Ahles, Denis Jacquemin, Nikos Tagmatarchis, Chris Ewels,* Hermann A. Wegner**

Page No. – Page No.

Electronic communication between two [10]cycloparaphenylenes and bisazafullerene $(C_{59}N)_2$ induced by cooperative complexation